Inorganic Chemistry

Article

pubs.acs.org/IC

Selective Synthesis of Ternary Copper–Antimony Sulfide Nanocrystals

Dongying Xu,[†,‡] Shuling Shen,[§] Yejun Zhang,[‡] Hongwei Gu,*[,†] and Qiangbin Wang*[,‡]

[†]Division of Chemistry and Materials, Soochow University, Suzhou 215123 People's Republic of China

[‡]Suzhou Key Laboratory of Nanomedical Characterization, Division of Nanobiomedicine and i-Lab, Suzhou Institute of Nano-Tech and Nano-Bionics, Chinese Academy of Sciences, Suzhou 215123 People's Republic of China

[§]School of Materials Science and Engineering, University of Shanghai for Science and Technology, Shanghai, 200093 People's Republic of China

Supporting Information

ABSTRACT: Ternary copper–antimony sulfide nanocrystals (CAS NCs) have attracted increasing attention in photovoltaics and photoelectric nanodevices due to their tunable band gaps in the near-IR regime. Although much progress in the synthesis of CAS NCs has been achieved, the selective synthesis of CAS NCs with controllable morphologies and compositions is preliminary: in particular, a facile method is still in demand. In this work, we have successfully selectively synthesized high-quality CAS NCs with diverse morphologies, compositions, and band gaps, including rectangular $CuSbS_2$ nanosheets (NSs), trigonal-pyramidal $Cu_{12}Sb_4S_{13}$ NCs, and rhombic Cu_3SbS_3 NSs, by cothermodecomposition of copper diethyldithiocarbamate trihydrate ($Cu(Ddtc)_2$) and antimony diethyldithiocarbamate trihydrate ($Sb(Ddtc)_3$). The direct and indirect band gaps of the obtained CAS NCs were systematically studied by performing Kubelka–Munk transformations of their solid-state diffuse reflectance spectra.

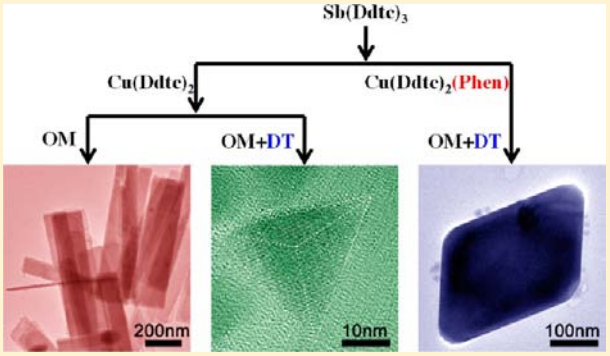

INTRODUCTION

As an efficient way to obtain new materials, the alloying of metal chalcogenide nanocrystals (NCs) with different chemical compositions and crystalline structures has attracted intense attention recently, due to their significance in fundamental studies and practical applications.[1−5] For example, ternary $CuInS_2$[6,7] and $AgFeS_2$[8] and quaternary Cu_2ZnSnS_4 NCs[9] have been engineered as very promising candidates for solar cell applications due to their suitable band gaps and high absorption coefficients to the solar light. $Cu_2CdSnSe_4$[10] and $Cu_2ZnSnSe_4$[11] have been observed with a relatively large power factor and figure of merit ZT which have the potential for important applications in cooling and power generation. In particular, ternary copper–antimony sulfide NCs (CAS NCs) have been the focus of recent research because of their tunable band gap energies in the near-IR regime, which are composition and crystal phase dependent. The past decade has witnessed the progress of controlled synthesis of CAS NCs.[12−14] However, despite the previously documented studies, the selective synthesis of CAS NCs with controllable morphologies and compositions is preliminary: in particular, a facile method is still in demand.

Among various solution-phase synthetic strategies, the thermodecomposition of a single-source precursor (SSP) method may be useful in addressing this challenge, since it has been proven facile and valid in obtaining a variety of metal chalcogenide NCs with the characteristics of single crystallites, pure phases, and monodispersities. O'Brien pioneered this facile synthetic process and first obtained CdS and CdSe NCs by using $Cd[E_2CN(C_2H_5)_2]_2$ as SSP (E = S, Se).[15,16] PbS,[17] ZnS, and ZnSe[18] were also successfully prepared using the SSP method with $Pb(S_2CNEtPr^i)_2$ and $Zn[E_2CNMe(C_6H_{13})]_2$ (E = S, Se) as precursors, respectively. Later on, Vittal and co-workers further extended this SSP method from preparing binary metal chalcogenides to ternary metal chalcogenides. For example, binary Ag_2Se NCs[19] and La_2S_3 film[20] and ternary $AgInS_2$ NCs[21] and $AgInSe_2$ nanorods[22] have been successfully obtained by employing $[(Ph_3P)_3Ag_2(SeCOPh)_2]$, $[La(bipy)(S_2CNEt_2)_3]$, and $[(Ph_3P)_2AgIn(ECOPh)_4]$ (E = S, Se) as SSPs, respectively. On the basis of these previous efforts, our group has also achieved controllable synthesis of binary metal sulfide NCs by using metal diethyldithiocarbamate trihydrate ($M(Ddtc)_x$, M = Ag, Zn, Sn, Mn, Fe, Cd) as a SSP.[23]

In this work, the facile SSP method was utilized to selectively synthesize high-quality CAS NCs with diverse morphologies and compositions with slight modification. Considering the complex synthetic procedure for preparing a SSP that contains the three elements copper, antimony, and sulfur, we employed a modified SSP method: that is, $Cu(Ddtc)_2$ and $Sb(Ddtc)_3$ as

Received: May 23, 2013
Published: October 31, 2013

dual sources were cothermodecomposed to prepare ternary CAS NCs. High-quality CAS NCs with diverse morphologies and compositions were successfully obtained, including rectangular $CuSbS_2$ nanosheets (NSs), trigonal-pyramidal $Cu_{12}Sb_4S_{13}$ NCs, and rhombic Cu_3SbS_3 NSs. Their optical properties were systematically characterized by solid-state optical diffuse reflectance spectroscopy, in which the direct and indirect band gaps of $CuSbS_2$ NSs, $Cu_{12}Sb_4S_{13}$ NCs, and Cu_3SbS_3 NSs were well-defined.

EXPERIMENTAL SECTION

Chemicals. Antimony(III) trichloride ($SbCl_3$, 99%), copper(II) chloride dihydrate ($CuCl_2{\cdot}2H_2O$, 99%), sodium diethyldithiocarbamate trihydrate ($Na(Ddtc){\cdot}3H_2O$, 99%), and1,10-phenanthroline ($(Phen){\cdot}H_2O$, 99%) were purchased from Sinopharm Chemical Reagent Co., Ltd. Oleylamine (OM; 70%, Fluka), 1-dodecanethiol (DT; 90%, ACROS), absolute ethanol, and cyclohexane were of analytical grade and were used as received without further purification.

Synthesis of $Sb(Ddtc)_3$ and $Cu(Ddtc)_2$. A 10 mmol portion (2.26 g) of $SbCl_3$ and 30 mmol (6.76 g) of $Na(Ddtc){\cdot}3H_2O$ were dissolved in absolute ethanol, respectively. Then, the two solutions were mixed with stirring in a 250 mL beaker. After constant stirring for 30 min, the reaction solution was kept stationary under ambient conditions for 2 h. The resulting yellow precipitate was filtered, washed with absolute ethanol and distilled water, and then dried in air at 60 °C. $Cu(Ddtc)_2$ was prepared by a method similar to that above, except that $SbCl_3$ and absolute ethanol were replaced by $CuCl_2{\cdot}2H_2O$ and deionized water.

Synthesis of $Cu(Ddtc)_2(Phen)$. A 10 mmol portion (2.00 g) of $(Phen){\cdot}H_2O$ was dissolved in boiling water. Then it was introduced into 10 mmol (1.71 g) of $CuCl_2{\cdot}2H_2O$ in aqueous solution with vigorous stirring. The solution mixture turned brown because of the reaction between Phen and copper ions. After 10 min, 20 mmol (4.51 g) of $Na(Ddtc){\cdot}3H_2O$ in aqueous solution was added dropwise into the above brown solution, and the aqueous solution turned turbid black. After 3 h, the resultant black precipitate was collected by vacuum filtration and washed with deionized water. The black precipitate was dried at 60 °C.

Synthesis of Rectangular $CuSbS_2$ NSs. The synthesis was carried out using an oxygen-free procedure. In a typical procedure, 0.1 mmol (0.056 g) of $Sb(Ddtc)_3$ and 0.1 mmol (0.036 g) of $Cu(Ddtc)_2$ were added into 44 mmol (10.8 g) of OM in a three-necked flask (100 mL) at room temperature. Then, the slurry was heated to 120 °C to remove water and oxygen with vigorous magnetic stirring under vacuum for 20 min in a temperature-controlled electric mantle. The solution was heated to 220 °C and kept for 1 h under an N_2 atmosphere. Then it was cooled naturally at room temperature. Afterward, the as-prepared NCs were purified by several centrifugation/dispersion cycles using cyclohexane/absolute ethanol (1/4 v/v).

Synthesis of Trigonal-Pyramidal $Cu_{12}Sb_4S_{13}$ NCs. The synthetic procedure of trigonal-pyramidal $Cu_{12}Sb_4S_{13}$ NCs was same as that of rectangular $CuSbS_2$ NSs, except that the solvent used here was an OM/DT mixture (OM/DT = 1/0.47, 120 mmol/56 mmol).

Synthesis of Rhombic Cu_3SbS_3 NSs. In a typical synthetic procedure, 0.1 mmol (0.056 g) of $Sb(Ddtc)_3$ and 0.1 mmol (0.054 g) of $Cu(Ddtc)_2(Phen)$ were added into a solvent mixture of OM and DT (OM/DT = 1/1.2, 20 mmol/24 mmol) in a three-necked flask (100 mL) at room temperature. The following procedure was same as that for rectangular $CuSbS_2$ NSs and trigonal-pyramidal $Cu_{12}Sb_4S_{13}$ NCs.

Characterization. The size, morphology, and high-resolution transmission electron microscopy (HR-TEM) characterizations were examined by a scanning electron microscope (SEM, Quanta 400FEG, and American FEI) and a Tecnai G2 F20 S-Twin TEM (FEI, USA) operated at 200 kV, respectively. The SEM and TEM sampling were prepared by dropping the cyclohexane containing CAS NCs onto the silicon wafer and copper grid, respectively, which were then dried naturally under ambient conditions. Powder X-ray diffraction (PXRD) patterns of the dried powders were recorded on a X'Pert-Pro MPD (Holland) with a slit of 1/2° at a scanning rate of 4° min^{-1}, using Cu Kα radiation (λ = 1.5418 Å). Optical diffuse reflectance measurements were performed at room temperature using a PE Lambda 750 UV spectrophotometer equipped with an integrating sphere attachment and $BaSO_4$ as the reference. The element contents of the presynthesized $Sb(Ddtc)_3$, $Cu(Ddtc)_2$, and $Cu(Ddtc)_2(Phen)$ were determined by elemental analysis on an Elementar Vario EL system (Germany).

RESULTS AND DISCUSSION

Figure 1a shows the typical scanning electron microscopy (SEM) and transmission electron microscopy (TEM) images of

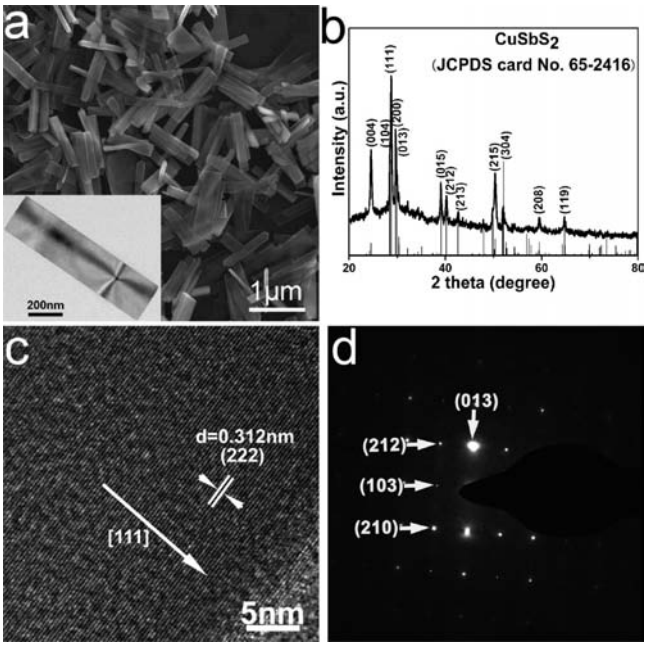

Figure 1. (a) SEM image, (b) XRD pattern, (c) HR-TEM image, and (d) SAED pattern of rectangular $CuSbS_2$ NSs. Inset in (a): TEM image of a single $CuSbS_2$ NS.

the products as rectangular NSs with a typical size of 200 × 850 nm. The XRD result in Figure 1b illustrates that all the diffraction peaks from the product can be indexed to the orthorhombic $CuSbS_2$ (JCPDS No. 65-2416, space group *Pnma* (No. 62), lattice parameters a = 6.02 Å, b = 3.79 Å, c = 14.49 Å; Figure S1 (Supporting Information)). The HR-TEM image of a selected region of the NS (Figure 1c) shows the perfect single-crystal structure of $CuSbS_2$ NSs. The measured lattice space is 0.312 nm for the lattice planes perpendicular to the axis of the NS, representing the (222) lattice plane of orthorhombic $CuSbS_2$. The selected area electron diffraction (SAED) pattern in Figure 1d further confirms the single-crystal nature of the $CuSbS_2$ NSs. These results demonstrate that rectangular single-crystal $CuSbS_2$ NSs with a typical size of 200 × 850 nm have been successfully obtained.

By changing the solvent from OM to a mixture of OM and DT (OM/DT = 1/0.47), while keeping other reaction conditions constant, single-crystal $Cu_{12}Sb_4S_{13}$ NCs were obtained. The TEM image in Figure 2a shows the trigonal-pyramidal $Cu_{12}Sb_4S_{13}$ NCs with an average side length of 30 nm. The inset in Figure 2a shows a magnified view, highlighting the three-dimensional morphology of the $Cu_{12}Sb_4S_{13}$ NCs. The XRD pattern in Figure 2b agrees well with the cubic $Cu_{12}Sb_4S_{13}$

dx.doi.org/10.1021/ic401291a | *Inorg. Chem.* 2013, 52, 12958−12962

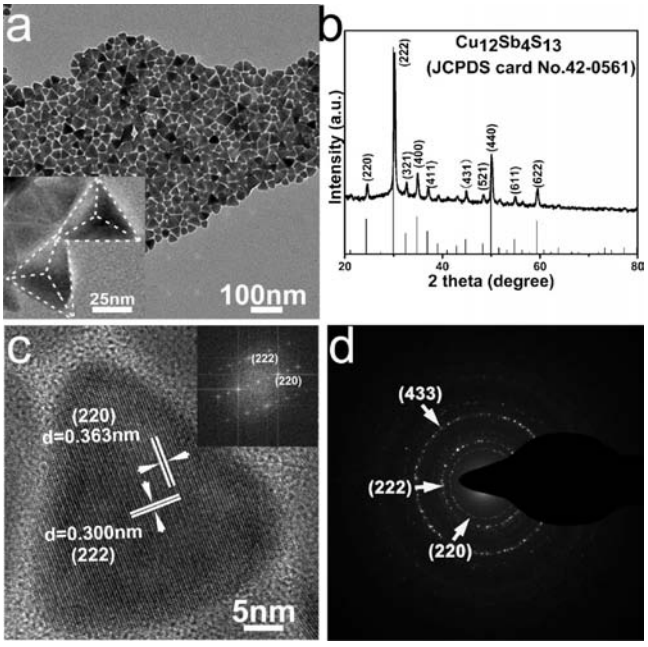

Figure 2. (a) TEM image, (b) XRD pattern, (c) HR-TEM image, and (d) SAED pattern of trigonal-pyramidal $Cu_{12}Sb_4S_{13}$ NCs. Inset in (a): a magnified view of $Cu_{12}Sb_4S_{13}$ NCs. Inset in (c): FFT pattern of a trigonal-pyramidal $Cu_{12}Sb_4S_{13}$ NC corresponding to the HR-TEM image.

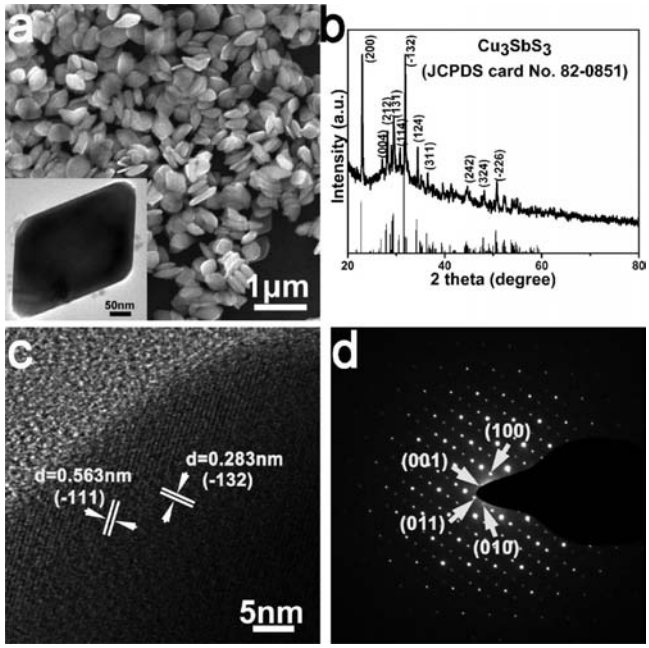

Figure 3. (a) SEM image, (b) XRD pattern, (c) HR-TEM image, and (d) SAED pattern of rhombic Cu_3SbS_3 NSs. Inset in (a): TEM image of a Cu_3SbS_3 NS.

(JCPDS No. 42-0561, space group $I\bar{4}3m$, lattice parameters $a = b = c = 10.323$ Å; Figure S2 (Supporting Information)). A HR-TEM image of a single trigonal-pyramidal $Cu_{12}Sb_4S_{13}$ NC is shown in Figure 2c, illustrating the single-crystal nature of the product with a lattice space of 0.3 nm, which matches well the lattice space between the (222) lattice planes of cubic $Cu_{12}Sb_4S_{13}$. The inset in Figure 2c is the corresponding FFT pattern of the obtained $Cu_{12}Sb_4S_{13}$ NCs, which further confirms the single-crystal nature of the trigonal-pyramidal $Cu_{12}Sb_4S_{13}$ NCs. Figure 2d presents the SAED pattern of $Cu_{12}Sb_4S_{13}$ NCs. There are three obvious diffraction rings assigned to the (220), (222), and (433) facets of the cubic $Cu_{12}Sb_4S_{13}$, which are consistent with the XRD pattern in Figure 2b. These results demonstrate that single-crystal trigonal-pyramidal $Cu_{12}Sb_4S_{13}$ NCs with a typical side length of 30 nm can be successfully obtained by using $Sb(Ddtc)_3$ and $Cu(Ddtc)_2$ as precursors and OM/DT as cosolvent, in which the addition of DT and a decreased amount of OM play important roles in determining the morphology and composition of the product.

We further changed the precursor of $Cu(Ddtc)_2$ to $Cu(Ddtc)_2(Phen)$ and decreased the amount of OM in the reaction from the mole ratio of OM to DT of 1/0.47 to 1/1.2; rhombic Cu_3SbS_3 NSs were obtained with a typical size of 200 × 300 nm, as shown in Figure 3a. The inset in Figure 3a presents the TEM image of rhombic Cu_3SbS_3 NSs. The XRD result in Figure 3b confirms the as-obtained Cu_3SbS_3 NSs in the monoclinic phase (JCPDS No. 82-0851, space group $P2_1/c$ (No. 14), lattice parameters $a = 7.808$ Å, $b = 10.233$ Å, $c = 13.268$ Å; Figure S3 (Supporting Information)). The HR-TEM image in Figure 3c shows the highly ordered crystal fringes which are ascribed to the (−132) and (−111) facets of monoclinic Cu_3SbS_3. The SAED pattern of rhombic Cu_3SbS_3 NS in Figure 3d demonstrates that the rhombic Cu_3SbS_3 NS is single crystalline, in which electron diffractions are in good accordance with the (100), (001), (011), and (010) planes of the Cu_3SbS_3 crystal structure. These results demonstrate that single-crystal rhombic Cu_3SbS_3 NSs with a typical size of 200 × 300 nm can be successfully obtained by using $Sb(Ddtc)_3$ and $Cu(Ddtc)_2(Phen)$ as precursors and OM/DT as cosolvents. These results further demonstrate the importance of ligands including Phen, OM, and DT, which affect the nucleation and growth process of the Cu_3SbS_3 NSs.

As shown above, the morphologies, compositions, and crystalline structures of the obtained CAS NCs can be conveniently adjusted. With OM as the only surfactant, rectangular $CuSbS_2$ NSs were obtained. It has been well documented that OM facilitates the growth of two-dimensional NCs by specifically binding to a certain crystal facet,[23−25] which determines the growth of $CuSbS_2$ NSs along the (111) direction in our case. DT was usually used as both the sulfur (S) source and surface capping ligand for the growth of metal sulfide nanocrystals.[26,27] Therefore, in the case of the reaction with the mole ratio of OM to DT as 1/0.47, DT provided supernumerary S and led to the formation of trigonal-pyramidal $Cu_{12}Sb_4S_{13}$ NCs. Further increasing the dosage of DT (the molar ratio of OM to DT was 1/1.2), irregularly shaped Cu_3SbS_3 nanostructures were obtained (see Figure S4 in the Supporting Information). However, when DT was used alone in the reaction system, no product was obtained because OM works not only as a stabilizer for the oriented growth of NCs but also as a catalyst for accelerating the decomposition of precursors; that is, OM controls the nucleation and growth kinetics of CAS NCs.[28,29] When $Cu(Ddtc)_2$ was replaced by $Cu(Ddtc)_2(Phen)$ in the reaction, the regularly rhombic Cu_3SbS_3 NSs were produced. The Phen ligand has been reported as an effective mediator in determining the growth kinetics of the nanocrystals.[25,30] In this study, we speculate that the Phen group decomposed from the precursor serves as the chelating ligand to strongly coordinate to the crystal facet, prohibiting subsequent growth along with the planes and

dx.doi.org/10.1021/ic401291a | Inorg. Chem. 2013, 52, 12958−12962

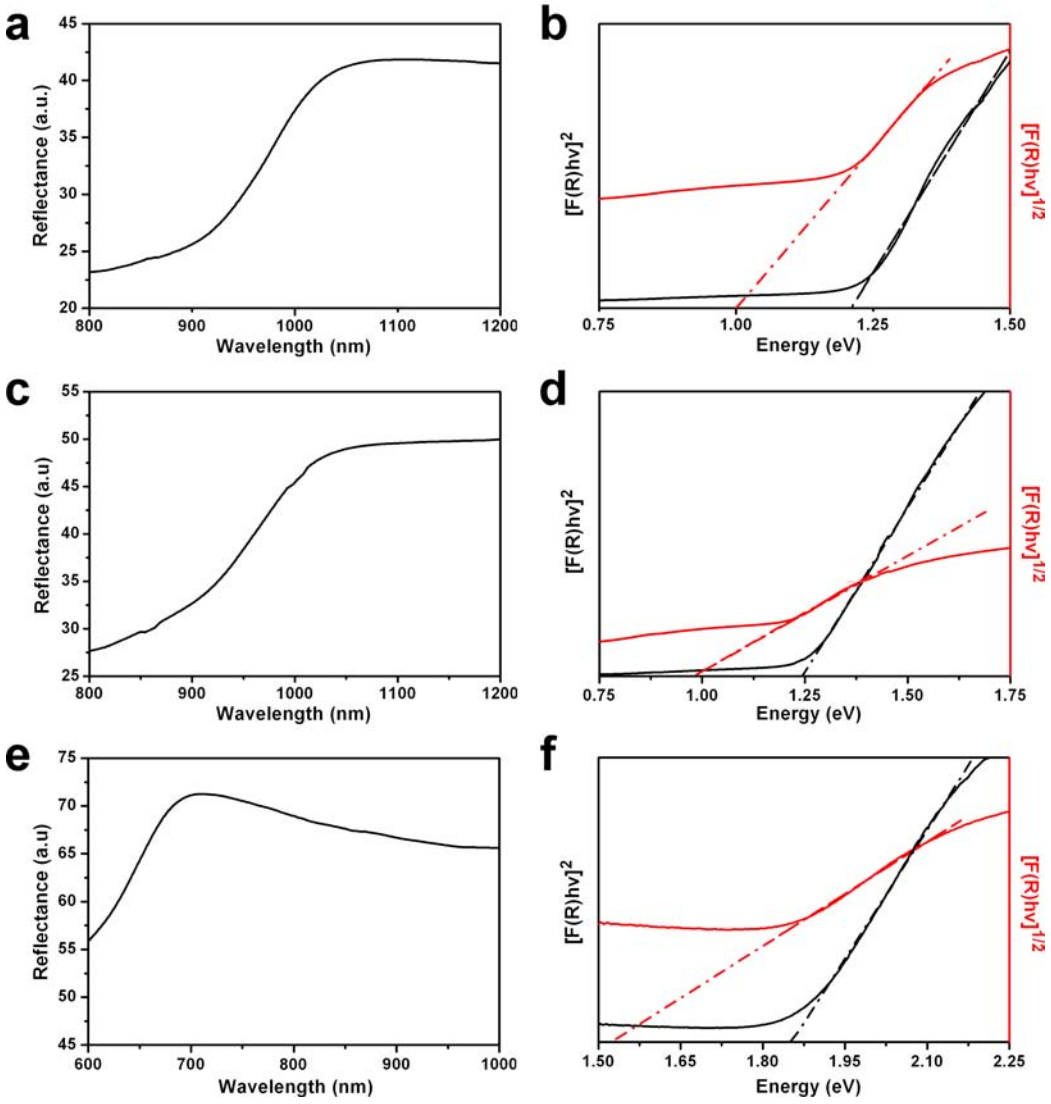

Figure 4. Solid-state optical diffuse reflectance spectra of (a) $CuSbS_2$ NSs, (c) $Cu_{12}Sb_4S_{13}$ NCs, and (e) Cu_3SbS_3 NSs and the calculated direct (black line) and indirect (red line) band gaps by Tauc plots of (b) $CuSbS_2$ NSs, (d) $Cu_{12}Sb_4S_{13}$ NCs, and (f) Cu_3SbS_3 NSs.

considerably influencing the crystallization process, and thus resulting in the rhombic Cu_3SbS_3 NSs. As illustrated above, using this facile method, well-defined CAS NCs with different compositions and shapes can be selectively synthesized by tuning the composition of solvents and precursors.

Since CAS NCs have been considered as ideal candidates for solar cells and photovoltaics due to their tunable band gaps in the near-IR regime, it is important to have a clear picture of the optical properties of the obtained $CuSbS_2$ NSs, $Cu_{12}Sb_4S_{13}$ NCs, and Cu_3SbS_3 NSs, which are composition and crystal phase dependent. Diffuse reflectance spectroscopy was subsequently performed to acquire the band gaps of the obtained CAS NSs. As shown in Figure 4, the onset absorptions of $CuSbS_2$ NSs and $Cu_{12}Sb_4S_{13}$ NCs are around 1000 nm (Figure 4a,c), while the onset absorption of Cu_3SbS_3 blue-shifts to around 700 nm (Figure 4e). By a Kubelka–Munk transformation,[31] the direct band gaps of $CuSbS_2$ NSs, $Cu_{12}Sb_4S_{13}$ NCs, and Cu_3SbS_3 NSs are 1.20, 1.24, and 1.85 eV and the indirect band gaps of $CuSbS_2$ NSs, $Cu_{12}Sb_4S_{13}$ NCs, and Cu_3SbS_3 NSs are 1.00, 0.98, and 1.52 eV, respectively (Figure 4b,d,f). Because of the large size of the obtained NCs, no quantum confinement effect was observed, and thus their direct bands are all in good agreement with the previous reports of bulk $CuSbS_2$,[32] $Cu_{12}Sb_4S_{13}$,[33] and Cu_3SbS_3.[34] It is notable that there has been less attention paid to the indirect band gap of CAS NCs; therefore, this work has first presented the indirect band gaps of $CuSbS_2$ NSs, $Cu_{12}Sb_4S_{13}$ NCs, and Cu_3SbS_3 NSs, in good complement to the literature.

■ CONCLUSION

In conclusion, we have successfully selectively synthesized a series of single-crystal CAS NCs (rectangular $CuSbS_2$ NSs, trigonal-pyramidal $Cu_{12}Sb_4S_{13}$ NCs, and rhombic Cu_3SbS_3 NSs) with uniform morphologies and pure crystalline phases by using a facile one-pot cothermodecomposition dual-precursor strategy. The crystalline phase, composition, morphology, and band gap of the products are readily obtained by changing the ligand molecules and precursors. The direct and indirect band gaps of the obtained CAS NCs were determined by performing Kubelka–Munk transformations. Their appropriate band gaps in the near-IR regime show that the obtained CAS NCs could have great potential in photovoltaics and photoelectric nanodevices. Furthermore, we expect that such a facile synthetic method could be extended to

dx.doi.org/10.1021/ic401291a | Inorg. Chem. 2013, 52, 12958–12962

the synthesis of other multinary metal sulfide NCs with desirable band gaps and optical properties.

■ ASSOCIATED CONTENT

Supporting Information

Text, a table, and figures giving compositions of the prepared precursors, unit cell patterns, additional TEM images, and band gap plots. This material is available free of charge via the Internet at http://pubs.acs.org..

■ AUTHOR INFORMATION

Corresponding Authors

*E-mail for H.G.: hongwei@suda.edu.cn.
*E-mail for Q.W.: qbwang2008@sinano.ac.cn

Notes

The authors declare no competing financial interest.

■ ACKNOWLEDGMENTS

We acknowledge funding by the Chinese Academy of Sciences Bairen Ji Hua Program, the National Natural Science Foundation of China (Grant Nos. 21073225, 21101166), the Natural Science Foundation of Jiangsu province (Grant No. BK2012007), and Guangxi Key Laboratory of Information Materials, Guilin University of Electronic Technology (1110908-02-K).

■ REFERENCES

(1) Kovalenko, M. V.; Scheele, M.; Talapin, D. V. *Science* **2009**, *324*, 1417.
(2) Li, S.; Zhao, Z.; Liu, Q.; Huang, L.; Wang, G.; Pan, D.; Zhang, H.; He, X. *Inorg. Chem.* **2011**, *50*, 11958.
(3) Regulacio, M. D.; Han, M. Y. *Acc. Chem. Res.* **2010**, *43*, 621.
(4) Peng, X. G. *Acc. Chem. Res.* **2010**, *43*, 1387.
(5) Malik, M. A.; Afzaal, M.; O'Brien, P. *Chem. Rev.* **2010**, *110*, 4417.
(6) Weil, B. D.; Connor, S. T.; Cui, Y. *J. Am. Chem. Soc.* **2010**, *132*, 6642.
(7) Li, L.; Coates, N.; Moses, D. *J. Am. Chem. Soc.* **2010**, *132*, 22.
(8) Han, S. K.; Gu, C.; Gong, M.; Wang, Z. M.; Yu, S. H. *Small* **2013**, DOI: 10.1002/smll.201300268.
(9) Lu, X. T.; Zhuang, Z. B.; Peng, Q.; Li, Y. *Chem. Commun.* **2011**, *47*, 3141.
(10) Fan, F. J.; Yu, B.; Wang, Y. X.; Zhu, Y. L.; Liu, X. J.; Yu, S.; Ren, Z. F. *J. Am. Chem. Soc.* **2011**, *133*, 15910.
(11) Fan, F. J.; Wang, Y. X.; Liu, X. J.; Wu, L.; Yu, S. *Adv. Mater.* **2012**, *24*, 6158.
(12) Wang, M. X.; Yue, G. H.; Fan, X. Y.; Yan, P. X. *J. Cryst. Growth* **2008**, *310*, 3062.
(13) van Embden, J.; Tachibana, Y. *J. Mater. Chem.* **2012**, *22*, 11466.
(14) An, C. H.; Jin, Y.; Tang, K.; Qian, Y. *J. Mater. Chem.* **2003**, *13*, 301.
(15) Trindade, T.; O'Brien, P. *J. Mater. Chem.* **1996**, *6*, 343.
(16) Trindade, T.; O'Brien, P.; Zhang, X. M. *Chem. Mater.* **1997**, *9*, 523.
(17) Trindade, T.; O'Brien, P.; Zhang, X. M.; Motevalli, M. *J. Mater. Chem.* **1997**, *7*, 1011.
(18) Ludolph, B.; Malik, M. A.; O'Brien, P.; Revaprasadu, N. *Chem. Commun.* **1998**, *34*, 1849.
(19) Ng, M. T.; Boothroyd, C. B.; Vittal, J. J. *Chem. Commun.* **2005**, *41*, 3820.
(20) Lu, T.; Ti, O. Y.; Loh, K. P.; Vittal, J. J. *J. Mater. Chem.* **2006**, *16*, 272.
(21) Lu, T.; Elim, H. I.; Ji, W.; Vittal, J. J. *Chem. Commun.* **2006**, *42*, 4276.
(22) Ng, M. T.; Boothroyd, C. B.; Vittal, J. J. *J. Am. Chem. Soc.* **2006**, *128*, 7118.
(23) (a) Du, Y. P.; Xu, B.; Fu, T.; Cai, M.; Li, F.; Zhang, Y.; Wang, Q. B. *J. Am. Chem. Soc.* **2010**, *132*, 1470. (b) Zhang, Y. J.; Lu, J.; Shen, S. L.; Xu, H. R.; Wang, Q. B. *Chem. Commun.* **2011**, *47*, 5226. (c) Zhang, Y. J.; Xu, H. R.; Wang, Q. B. *Chem. Commun.* **2010**, *46*, 8941. (d) Shen, S. L.; Zhang, Y. J.; Peng, L.; Du, Y. P.; Wang, Q. B. *Angew. Chem., Int. Ed.* **2011**, *50*, 7115. (e) Shen, S. L.; Zhang, Y. J.; Liu, Y. S.; Peng, L.; Chen, X. Y.; Wang, Q. B. *Chem. Mater.* **2012**, *24*, 2407.
(24) Son, J. S.; Wen, X. D.; Joo, J.; Chae, J.; Baek, S. I.; Park, K.; Kim, J. H.; An, K.; Yu, J. H.; Kwon, S. G.; Choi, S. H.; Wang, Z. W.; Kim, Y. W.; Kuk, Y.; Hoffmann, R.; Hyeon, T. *Angew. Chem., Int. Ed.* **2009**, *48*, 6861.
(25) Li, L.; Chen, Z.; Hu, Y.; Wang, X. W.; Zhang, T.; Chen, W.; Wang, Q. B. *J. Am. Chem. Soc.* **2013**, *135*, 1213.
(26) Zhuang, Z.; Peng, Q.; Wang, X.; Li, Y. *Angew. Chem., Int. Ed.* **2007**, *46*, 8174.
(27) Ramasamy, K.; Mazumdar, D.; Zhou, Z. Y.; Wang, Y. H. A.; Gupta, A. *J. Am. Chem. Soc.* **2011**, *133*, 20716.
(28) Kwon, S. G.; Hyeon, T. *Acc. Chem. Res.* **2008**, *41*, 1696.
(29) Mourdikoudis, S.; Liz-Marzan, L. M. *Chem. Mater.* **2013**, *25*, 1465.
(30) Mirkovic, T.; Hines, M. A.; Nair, P. S.; Scholes, G. D. *Chem. Mater.* **2005**, *17*, 3451.
(31) Hagfeldt, A.; Gratzel, M. *Chem. Rev.* **1995**, *95*, 49.
(32) Rabhi, A.; Kanzari, M. *Chalcogenide Lett.* **2011**, *8*, 255.
(33) Bullett, D. W.; Dawson, W. G. *J. Phys. C: Solid State Phys.* **1986**, *19*, 5837.
(34) Maiello, P.; Zoppi, G.; Miles, R. W.; Pearsall, N.; Forbes, I. *Investigations of Ternary Cu_3BiS_3 Thin Films as Absorber in Photovoltaic Devices*, 7th Photovoltaic Science, Applications, and Technology Conference C93, PVSAT-7, Edinburgh, Scotland, April 6−8, 2011.